

RESEARCH

Open Access



# Variability and variation in *Rhyncholestes raphanurus* Osgood (Paucituberculata, Caenolestidae)

Baltazar González<sup>1</sup>, Federico Brook<sup>1,2</sup> and Gabriel M. Martín<sup>1,2\*</sup>

## Abstract

**Background:** Caenolestids are a group of poorly known South American marsupials with a restricted distribution in *Páramo* and *Subpáramo* environments of the Andes from Colombia and western Venezuela to Bolivia (represented by the genera *Caenolestes* and *Lestoros*), and Valdivian rainforest in southern Chile (including a separate population in Chiloé Island) and Argentina, where a single species lives: the Long-nosed shrew opossum (*Rhyncholestes raphanurus*). The objectives of this work were to analyze the intraspecific variability of *R. raphanurus*, which includes an anatomical description of the skull and dentition, describe its geographic variation, test for sexual dimorphism, and assess potential differences between continental and Island populations.

**Methods:** Linear Mossimann-transformed variables were used to assess sexual differences within a large population (La Picada), compare sexes within other continental populations, and in a separate analysis, compare continental from Island samples. A full model Principal Components Analysis was performed to assess differences between males and females of the continental and Island populations. A thorough description of the skull and teeth of the species and comparisons with other living Caenolestidae is presented.

**Results:** *Rhyncholestes raphanurus* presents little geographic variation, even between Island and continental populations. Similarly, we found no significant difference between sexes of this species in cranial and dental measurements. We provide a detailed description of cranial morphology and its variation, and also, the first description of the occipital bones, which haven't been previously described for any Paucituberculata.

**Conclusions:** Comparative studies of continental and Chiloé Island specimens support the treatment of *R. raphanurus* as a single valid species, especially since morphologic and morphometric differences fall within the extremes of continental populations. The morphology of *R. raphanurus* clearly separates this genus from other extant Caenolestidae, and in a much greater degree than the differences found between *Lestoros* and *Caenolestes*.

**Keywords:** Chiloé Island, Continental Chile, Craniodental morphology, Sexual dimorphism

\* Correspondence: [gmartin\\_ar@yahoo.com](mailto:gmartin_ar@yahoo.com)

<sup>1</sup>Centro de Investigación Esquel de Montaña y Estepa Patagónica (CIEMEP), Consejo Nacional de Investigaciones Científicas y Técnicas (CONICET) – Universidad Nacional de la Patagonia “San Juan Bosco” (UNPSJB), Esquel, Chubut, Argentina

<sup>2</sup>Laboratorio de Investigaciones en Evolución y Biodiversidad. Facultad de Ciencias Naturales y Ciencias de la Salud. Sede Esquel, UNPSJB, Esquel, Chubut, Argentina



© The Author(s). 2020 **Open Access** This article is licensed under a Creative Commons Attribution 4.0 International License, which permits use, sharing, adaptation, distribution and reproduction in any medium or format, as long as you give appropriate credit to the original author(s) and the source, provide a link to the Creative Commons licence, and indicate if changes were made. The images or other third party material in this article are included in the article's Creative Commons licence, unless indicated otherwise in a credit line to the material. If material is not included in the article's Creative Commons licence and your intended use is not permitted by statutory regulation or exceeds the permitted use, you will need to obtain permission directly from the copyright holder. To view a copy of this licence, visit <http://creativecommons.org/licenses/by/4.0/>.

## Background

Caenolestids are usually considered some of the least known Neotropical mammals [1], and due to the lack of comprehensive morphological studies the extent of variability and variation within its species is little known. Extant species of the family Caenolestidae (order Paucituberculata) are small terrestrial marsupials with a distribution along the Andean region of South America, from Colombia and Venezuela to Chile [2]. Three genera are currently recognized within Caenolestidae: *Caenolestes*, with five described species living in the high Andean ecosystems of the northern Andes of northern Perú, Ecuador, Colombia, and southwestern Venezuela; *Lestoros*, with a single species (*L. inca*) living in the high Andean ecosystems of southern Perú and northern Bolivia; and *Rhyncholestes*, with a single species (*R. raphanurus*) living in the Valdivian rainforest of Chile and Argentina [2, 3]. Although some of its species have a relatively wide distribution (e.g., *R. raphanurus*, *C. fuliginosus*, and *L. inca*), studies that incorporate the intraspecific variation and variability sensu [4] of extant Caenolestidae are scarce but see [5–8].

*Rhyncholestes raphanurus* was described by Osgood [9] in a review of living Caenolestids, based on specimens trapped in Chiloé Island, Chile. In this work, Osgood [9] compared the new species with *Caenolestes* and *Lestoros*, and noted the unique characters of *R. raphanurus* which includes a longer rostrum, bicuspid incisors, sexually dimorphic canines (caniniform in males, pre-molariform or double-rooted in females), 22 caudal vertebrae instead of 27 as in *Caenolestes*, and other external differences (e.g., short and seasonally incrassated tail, small eyes). Additionally, Osgood [9] anticipated the presence of this species in continental Chile, which was later confirmed by individuals trapped by Sanborn in 1939 (a single adult male), and Gallardo [10].

*Rhyncholestes raphanurus* is a small marsupial (males: < 45 g and females: < 38 g) with a mean body length (including the tail) of 189 and 185 mm for males and females, respectively [6, 11]. Ecological studies suggest nightly habits [6, 12, 13], and a diet with a high proportion of insects which also includes fungi and seeds [6]. Reproductively active females have been captured only during summer, while males seem to be active throughout the year [12]. As other austral marsupial species (e.g., *Lestodelphys halli*, *Dromiciops gliroides*), *R. raphanurus* seasonally stores fat in its tail, a trait that has been related to extended torpor [6, 14]. Although sometimes considered as a rare species [6, 9], it has been readily captured locally and is seasonally abundant at some places as La Picada (41° 06' S, 72° 30' W) [12, 13, 15]. Its known distribution ranges from 40°S to 42°S in the continent, but extends to 43°20'S in Chiloé Island [3, 11, 15], with ecological niche models suggesting a wider

distribution [3]. Few molecular studies about this species exist and are mainly focused on inter ordinal marsupial evolution e.g., [16] or intra-family phylogenetics [17]. Despite its importance as the southernmost extant Caenolestidae, little is known of the species' intraspecific morphologic and morphometric variability and variation.

In this context, questions about the geographical variation along the species' distribution remain unsolved. For example, Bublitz [18] accounted for this geographic variation separating *Rhyncholestes* in two species (a continental form, *R. continentalis*, and an insular form, *R. raphanurus*), using differences in the shape of female upper canines. However, Martin [11] and Patterson [19] considered this trait to be insufficient to separate the species, since only a single female from Chiloé was studied. Accordingly, posterior studies have treated this species as monotypic with two subspecies: the continental form, *R. raphanurus continentalis*, and the insular form, *R. r. raphanurus* [1, 2, 7, 11, 20], but comprehensive analyses of this are still lacking. A similar distinction between continental and Island forms was proposed for the marsupial *Dromiciops gliroides* [see 11 for a detailed account], but discarded based on morphology [7] and molecular analyses [21].

Other sources of variation for the species have not been assessed yet. For example, data from *C. fuliginosus* suggest that there is sexual variation among cranial, dental, and external traits [8, 22, 23], while for *L. inca* dimorphism is restricted only to external characters [7]. In contrast, information about sexual dimorphism in *R. raphanurus* remains restricted to qualitative [9, 18] or few external measurements (i.e., weight and body length [6, 11, 18]).

In this study, we focus on the variability and variation of craniodental characteristics following the approach recently used by Martin [24], in which variability was used to describe continuous, mostly intrapopulation character differences, while variation was used to describe different states of a certain character (i.e., polymorphic) between individuals in a sample (e.g., population, species in a clade) [4, 25–28]. By describing, analyzing, and comparing intraspecific or intrapopulation variability, we provide a framework to interpret interspecific variation between characters, which might be useful when comparing other Caenolestid species.

The aims of our study were to describe the variability and variation of *R. raphanurus*, testing for sexual dimorphism, the distinction between continental and insular forms, and the existence of latitudinal (clinal) variability. Due to the paucity of information for this species, we also present a detailed description of the skull and dentition.

## Methods

### Sample and variables

In this study, we analyzed the variability and variation of cranial, mandibular, and dental characters based on 77

specimens (including the holotype) of *R. raphanurus* (see Appendix 1) deposited in the following collections: AMNH, American Museum of Natural History, New York; BMNH, British Museum of Natural History, London; FMNH, Field Museum of Natural History, Chicago; MACN, Museo Argentino de Ciencias Naturales “Bernardino Rivadavia,” Buenos Aires; MMP, Museo de Mar del Plata “Lorenzo Scaglia,” Mar del Plata; UACH, Universidad Austral de Chile, Valdivia; and USNM, National Museum of Natural History, Smithsonian Institution, Washington, D.C.

External measurements for each specimen were registered from skin tags or field catalogs, and include total length (TTL), head-body length (HBL), tail length (TL), ear length (E), and hind foot length (F). When head-body length was not provided, it was calculated by subtracting TL to TTL. When TTL was not provided, it was calculated by adding HBL to TL.

We followed Wible [29] for skull anatomy except for the palate for which we follow Voss and Jansa [30]. Dental nomenclature was described according to Abello [31, 32], and dental homologies followed Luckett and Hong [33]. Upper and lower teeth are indicated by uppercase and lowercase letters, respectively. Therefore, teeth found in adult dentition of caenolestids are designated as follows: upper and lower incisors, I1–4 and i1–3 (from anterior to posterior); canines, C1 and c1; premolars, dP1–2 and dp1–2, and P3 and p3; molars, M1–4 and m1–4. The single functional deciduous tooth in each jaw quadrant is designated as dP3 or dp3, while the first two upper and lower premolars are considered unreplaced deciduous teeth as described by Luckett and Hong [33]. Lower teeth between the procumbent incisor (i.e., numerical i1) and the first identifiable lower premolar (dp2) are referred as “incisor-like teeth” (see Luckett and Hong [33] for a discussion on first lower incisor homologies). Special attention was focused on the morphology of the upper canine, since this tooth has been described as expressing sexual dimorphism [6, 9].

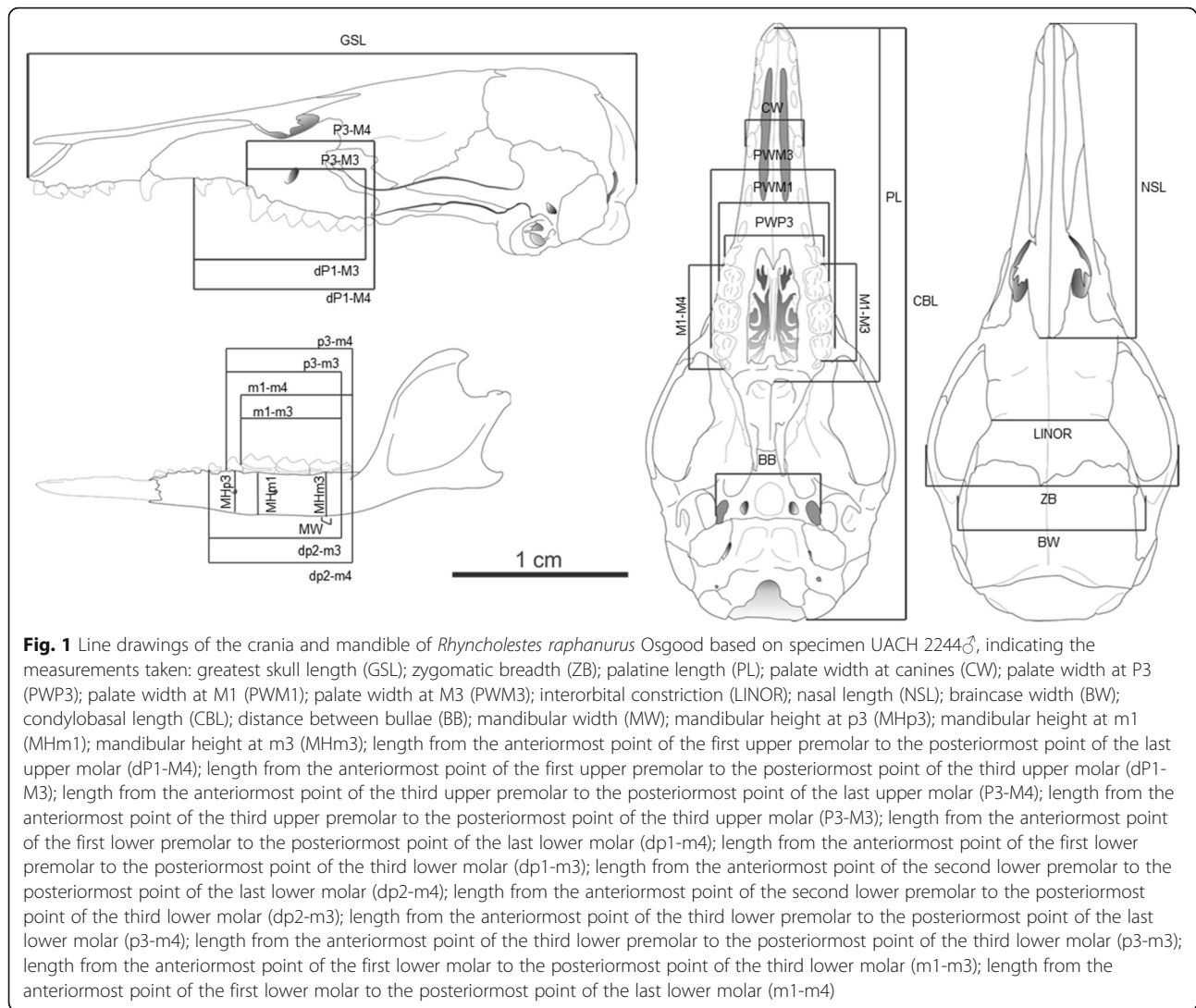
We took 36 linear measurements of crania, mandibles, and teeth of adult specimens (as indicated by completed tooth eruption) following Martin [7]: greatest skull length (GSL); zygomatic breadth (ZB); palatine length (PL); palate width at canines (CW); palate width at P3 (PWP3); palate width at M1 (PWM1); palate width at M3 (PWM3); interorbital constriction (LINOR); nasal length (NSL); braincase width (BW); condylobasal length (CBL); distance between bullae (BB), mandibular width (MW); mandibular height at p3 (MHp3); mandibular height at m1 (MHm1); mandibular height at m3 (MHm3), length from the anteriormost point of the first upper premolar to the posteriormost point of the last upper molar (dP1-M4); length from the anteriormost point of the first upper premolar to the posteriormost

point of the third upper molar (dP1-M3); length from the anteriormost point of the third upper premolar to the posteriormost point of the last upper molar (P3-M4); length from the anteriormost point of the third upper premolar to the posteriormost point of the third upper molar (P3-M3); length from the anteriormost point of the first lower premolar to the posteriormost point of the last lower molar (dp1-m4); length from the anteriormost point of the first lower premolar to the posteriormost point of the third lower molar (dp1-m3); length from the anteriormost point of the second lower premolar to the posteriormost point of the last lower molar (dp2-m4); length from the anteriormost point of the second lower premolar to the posteriormost point of the third lower molar (dp2-m3); length from the anteriormost point of the third lower premolar to the posteriormost point of the last lower molar (p3-m4); length from the anteriormost point of the third lower premolar to the posteriormost point of the third lower molar (p3-m3); length from the anteriormost point of the first lower molar to the posteriormost point of the third lower molar (m1-m3); length from the anteriormost point of the first lower molar to the posteriormost point of the last lower molar (m1-m4); length and width of first upper (LM1, WM1) and lower molars (Lm1, Wm1); length and width of third upper molar (LM3, WM3) (Fig. 1).

#### Data analysis

Since specimens were sample from several scattered localities, we pooled some of them according to their proximity and to increase the number of measured specimens. For continental samples ( $n = 59$ ), pooled localities were: (1) Entre Lagos-Puyehue National Park ( $n = 6$ ), (2) La Picada-V. Perez Rosales National Park ( $n = 48$ ), and (3) Contao ( $n = 5$ ); while for Chiloé samples ( $n = 12$ ) we used (4) Fundo El Venado ( $n = 9$ ), and (5) Puerto Cármen-Río Inio ( $n = 3$ ) (see Appendix I, Tables 1 and 2, and Martin [3] for localities). Six specimens could not be included in the analyses because they were damaged (i.e., not complete), or because they come from a locality which was not close enough to be pooled with others (e.g., Maicolpué).

Measurements of adult specimens were used to assess intraspecific variability, including possible sexual dimorphism and geographic variation, such as isolated populations (i.e., continental vs. insular forms) and geographic “clinal” variation. Linear measurements were converted to Mosimann variables by dividing individual measurements by the geometric mean of the measurements of all studied specimens [35]. In this way, shape variables (independent of size) were calculated and used in the different sexual dimorphism, geographic variation, and Principal Component Analysis (PCA; see below).



This methodology was previously used by Meachen-Samuels and Van Valkenburgh [36], Morales and Giannini [37], Schiaffini et al. [38], and Martin [24], because it provides a mean to test for differences in shape regardless of whether small and large adult individuals are included in the sample [35].

We proceeded from a local (i.e., a single locality, La Picada) to an inclusive approach (i.e., including all continental and Island specimens) to test for sexual dimorphism. A non-parametric Kruskal-Wallis analysis of variance (ANOVA) was performed to test for sexual dimorphism at La Picada, the single locality with the largest sample ( $n = 45$ ), followed by the same analysis including all continental samples. The same type of ANOVA was performed to test for differences between insular and continental forms (i.e., the distinction between *R. raphanurus raphanurus* and *R. raphanurus continentalis*).

To assess the significance of the non-parametric ANOVAs, we used a sequential Bonferroni correction following Rice [39], where  $p$ -values for external and craniodental variables (treated separately) were ranked from lowest to highest, and corrected  $p$ -values were calculated for each variable with the formula  $\alpha_1 = \alpha/k$ ,  $\alpha_2 = \alpha/k-1 \dots \alpha_i = \alpha$ , where  $\alpha_i$  is the corrected  $p$ -value for each comparison,  $\alpha$  is the alpha level to reject the null hypothesis, and  $k$  is the number of tests made. Sequential Bonferroni-corrected values at  $p = 0.05$  are shown in a separate column of Tables 3, 4 and 5. All statistical analyses were performed using InfoStat [40].

To explore the overall variability within the sample, we performed a full model PCA with the unconverted measurements and all the studied variables. Then, we used Mosimann converted measurements to explore the shape differences between all individuals, by performing three PCA: (1) including all external measurements; (2)

only using cranial measurements, and (3) only with dental measurements. These PCA were performed to test for intraspecific dispersion in three different modules of variation (i.e., external measurements, crania, teeth), and to include specimens from localities scattered throughout the species range which could not be analyzed using the non-parametric ANOVAs (see below). The number of Principal Components used were selected following Cattell [41]. The existence of clinal variability was tested by regressing latitude with the first two axes from each PCA [7].

Finally, to assess the variability and variation we present a detailed description of the skull and dentition of *Rhyncholestes raphanurus*, by accounting for geographic and sexual differences (see section “General structure of the cranium and mandibles”).

## Results

We studied a total of 77 specimens of *R. raphanurus* which came from several scattered localities throughout the species range, with a single locality (La Picada) producing 58.4% of the specimens (Appendix 1). Individuals were collected in continental Chile ( $n = 62$ ), a single continental locality in Argentina ( $n = 2$ ), and Chiloé Island ( $n = 14$ ) where the type specimen comes from [3, 9]. Of these, 48 (61.5%) were males, 29 (37.2%) were females and 1 specimen (1.3%) had indeterminate sex. The total number of specimens measured for each locality (or pooled locality), mean, SD, minimum and maximum of each variable, and coefficient of variation (CV) are presented in Tables 1 and 2.

### Intraspecific morphometric variability and variation

We found no significant differences between sexes in any external, craniomandibular and dental measurements analyzed for the locality with the largest number of specimens (La Picada) (Table 3). Also, no significant differences between sexes were found when all continental specimens were pooled together (Table 4). When comparing continental with Chiloé specimens, no significant differences were found in external, craniomandibular and most dental measurements, with the exception of palate width at M3 and length of M1-M3, different at  $p = 0.05$  sequential Bonferroni corrected values ( $p = 0.0012$  and  $p = 0.0014$ , respectively; Table 5). Craniodental measurements provided the least within-group variation, with the lowest coefficient of variation (CV) values.

The first 2 PCs explained 49% of the total variance of the full model PCA, and only included 43 (55%) of the 77 available specimens (Additional file 1). In the PCA for external, only cranial and only dental analyses, the first 2 PCs explained 74%, 85%, and 54% of the total variance, respectively. No significant trend was found

when the first 2 PCs were regressed with latitude for any set of variables, indicating no evidence for clinal variation (external measurements:  $n = 73$ ; PC1,  $r^2 = 0.04$ ,  $F = 0.47$ ,  $P = 0.8280$ ; PC2,  $r^2 = 0.17$ ,  $F = 2.27$ ,  $P = 0.047$ ; cranial measurements:  $n = 45$ ; PC1,  $r^2 = 0.14$ ,  $F = 1.06$ ,  $P = 0.4006$ ; PC2,  $r^2 = 0.24$ ,  $F = 1.98$ ,  $P = 0.0932$ ), with the exception of PC1 for dental measurements ( $n = 52$ ; PC1,  $r^2 = 0.47$ ,  $F = 6.76$ ,  $P = 0.0001$ ; PC2,  $r^2 = 0.1$ ,  $F = 0.85$ ,  $P = 0.5383$ ). These results show there is no significant morphometric differentiation between continental and insular specimens of *R. raphanurus*, with a clinal size variation in dental measurements, adding support to consider the species as the only living representative of the genus *Rhyncholestes*.

### General structure of the cranium and mandibles

The skull of *R. raphanurus* is similar to that of other Caenolestidae, but with a longer and more elongated rostrum, moderately expanded zygomatic arches, reduced orbits, a broad interorbital region, long, low and straight (i.e., not ventrally inflexed) mandibles, laterally compressed and “bilobed” upper incisors 2, 3 and 4; thin, very long and notoriously procumbent first lower incisors [9].

### Cranium

In dorsal view, nasals are parallel and present a lateral expansion posterior to the premaxillary-maxillary suture, with very large anteorbital vacuities. Anteorbital vacuities (AOV) are formed by the maxillary, nasal and frontal bones. These AOV are greatly varied in their development (size) and ossification, this variability being independent of sex and geographic locality. The most common state of the AOV is an open fenestra with the nasal forming dendritic patterns in its interior; however, sometimes AOV can present a thin ossified bone covering all of it or in others it can be completely ossified (Fig. 2). The latter pattern was only found unilaterally, i.e., one of the AOV was open and the other completely closed (Fig. 2). Nasals join the frontals forming an anteriorly open, well formed “U”. The posterior end of the nasals varies from anterior to the lacrimal foramen to posterior to this foramen, reaching a point in line with StC + D of M3. Frontals are the largest bones in the skull roof, with inflated frontal sinuses as wide as the interlacrimar width, a moderately developed postorbital constriction, anterior to the expansion that forms most of the brain cavity, mostly formed by the parietals dorsally, squamosal and alisphenoid laterally, and occipitals posteriorly. Normally, supraorbital processes and/or crests are not well developed in either frontals or parietals. However, very large specimens with highly worn teeth present small, though well-marked sagittal crests (e.g., UACH 4000♂, FMNH 22423♂). The contact between frontals and parietals is straight (i.e., transversal to the

**Table 1** External and craniodental measurements of *Rhyncholestes raphanurus* Osgood, for pooled samples from continental Chile. Total number of specimens (*n*), mean (*X*), *SD*, minimum and maximum of each variable, and coefficient of variation are presented for each locality. Asterisks mark Coefficient of Variation (CV) values higher than seven, following Bedeian and Mossholder [34]

Variables	Entre Lagos – Puyehue National Park			La Picada – V. Perez Rosales National Park			Contao (continental Chiloé)		
	<i>n</i>	<i>X</i> ± <i>SD</i> (min - max)	CV	<i>n</i>	<i>X</i> ± <i>SD</i> (min - max)	CV	<i>n</i>	<i>X</i> ± <i>SD</i> (min - max)	CV
TTL	6	191.08 ± 14.22 (176–215)	7.44*	48	187.53 ± 13.14 (159–215)	7.01*	5	187.4 ± 9.13 (180–203)	4.87
HBL	6	107.58 ± 9.55 (99–124)	8.88*	48	105.78 ± 10.81 (79–130.5)	10.22*	5	105.8 ± 8.87 (99–120)	8.38*
TL	6	83.5 ± 5.61 (77–91)	6.72	48	81.75 ± 7.55 (52.5–98)	9.24*	5	81.6 ± 3.97 (76–87)	4.87
E	6	12.42 ± 0.86 (11.5–14)	6.94	48	12.31 ± 0.93 (10–15)	7.57*	5	10 ± 1 (9–11)	10*
F	6	22.25 ± 1.44 (20–23.5)	6.47	47	21.48 ± 1.65 (17–25)	7.67*	5	21.3 ± 0.97 (20.5–23)	4.58
GSL	6	32.39 ± 1.78 (30.2–35.2)	5.5	32	32.39 ± 1.1 (30–35)	3.41	5	32.01 ± 0.83 (31.52–33.45)	2.58
ZB	6	13.42 ± 0.81 (12.5–14.7)	6.01	32	13.14 ± 0.6 (12.22–15.21)	4.55	5	12.91 ± 0.35 (12.55–13.49)	2.71
PL	6	19.47 ± 1.21 (18–20.9)	6.22	33	19.17 ± 0.75 (17.7–21.06)	3.89	5	19.24 ± 0.55 (18.8–20.14)	2.85
CW	6	3.07 ± 0.18 (2.9–3.4)	5.95	33	3.06 ± 0.13 (2.79–3.4)	4.37	5	2.99 ± 0.12 (2.82–3.12)	4.06
PWP3	3	5.32 ± 0.04 (5.28–5.36)	0.73	13	5.12 ± 0.15 (4.93–5.49)	3.01	5	4.94 ± 0.19 (4.65–5.18)	3.94
PWM1	6	6.2 ± 0.23 (5.8–6.4)	3.68	32	6.06 ± 0.17 (5.79–6.4)	2.79	5	5.84 ± 0.12 (5.69–5.99)	2.06
PWM3	6	6.99 ± 0.22 (6.6–7.21)	3.18	33	6.86 ± 0.15 (6.6–7.21)	2.24	5	6.89 ± 0.16 (6.65–7.01)	2.35
LINOR	6	6.85 ± 0.18 (6.5–7)	2.66	34	6.97 ± 0.18 (6.6–7.3)	2.57	5	7.07 ± 0.11 (6.93–7.24)	1.62
NL	6	17.2 ± 1.4 (15.2–18.5)	8.16*	33	16.94 ± 0.81 (15.3–18.7)	4.77	5	17.15 ± 0.47 (16.59–17.88)	2.73
BW	6	11.77 ± 0.46 (11–12.14)	3.95	33	11.6 ± 0.32 (10.8–12.55)	2.74	5	11.52 ± 0.3 (11.18–11.89)	2.62
CBL	6	29.95 ± 1.97 (27.6–32.8)	6.59	30	29.59 ± 1.13 (27.97–32.44)	3.81	5	29.55 ± 0.88 (29.01–31.12)	2.99
BB	6	5.43 ± 0.16 (5.2–5.6)	2.91	32	5.38 ± 0.22 (4.9–5.89)	4.11	5	5.5 ± 0.16 (5.33–5.77)	2.97
MW	6	1.11 ± 0.11 (1–1.3)	9.91*	34	1.08 ± 0.09 (0.9–1.27)	8.57*	5	1.07 ± 0.09 (0.99–1.22)	8.44*
MHp3	3	2.34 ± 0.07 (2.26–2.39)	2.88	14	2.15 ± 0.18 (1.93–2.59)	8.53*	5	2.05 ± 0.12 (1.91–2.18)	5.77
MHm1	3	1.97 ± 0.29 (1.8–2.3)	14.68*	20	2.05 ± 0.12 (1.9–2.3)	6.03	–	–	–
MHm3	3	2.21 ± 0.09 (2.13–2.31)	4.14	14	2.07 ± 0.14 (1.85–2.46)	6.99	5	1.98 ± 0.06 (1.93–2.08)	3.14
dP1 - M3	6	9.76 ± 0.41 (9.2–10.21)	4.24	34	9.71 ± 0.28 (8.8–10.21)	2.92	5	9.51 ± 0.19 (9.35–9.8)	1.95
dP1 - M4	6	10.14 ± 0.37 (9.6–10.6)	3.67	34	10.1 ± 0.29 (9.1–10.6)	2.87	5	9.9 ± 0.13 (9.78–10.08)	1.29
P3 - M3	6	6.41 ± 0.21 (6–6.6)	3.35	34	6.46 ± 0.17 (6.1–6.71)	2.59	5	6.33 ± 0.15 (6.17–6.55)	2.29
P3 - M4	6	6.83 ± 0.28 (6.3–7.1)	4.03	34	6.86 ± 0.17 (6.4–7.2)	2.49	5	6.71 ± 0.07 (6.63–6.81)	1.05
M1 - M3	6	5.22 ± 0.08 (5.1–5.33)	1.48	34	5.19 ± 0.16 (4.8–5.4)	2.99	5	5.15 ± 0.06 (5.08–5.23)	1.12
M1 - M4	6	5.65 ± 0.13 (5.4–5.74)	2.24	34	5.62 ± 0.16 (5.1–5.9)	2.92	5	5.58 ± 0.03 (5.54–5.61)	0.52
LM1	6	1.85 ± 0.1 (1.7–2.01)	5.68	34	1.9 ± 0.1 (1.7–2.1)	5.25	5	1.87 ± 0.01 (1.85–1.88)	0.74
WM1	6	1.45 ± 0.07 (1.32–1.5)	4.88	34	1.44 ± 0.07 (1.2–1.6)	5.17	5	1.41 ± 0.05 (1.37–1.47)	3.27
LM3	3	1.57 ± 0.06 (1.5–1.6)	3.74	14	1.58 ± 0.06 (1.47–1.7)	3.54	5	1.53 ± 0.04 (1.5–1.6)	2.73
WM3	3	1.43 ± 0.04 (1.4–1.47)	2.71	14	1.38 ± 0.04 (1.3–1.42)	3.18	5	1.39 ± 0.02 (1.37–1.42)	1.53
dp1 - m3	3	8.2 ± 0.3 (7.9–8.5)	3.66	20	8.34 ± 0.26 (7.6–8.8)	3.14	–	–	–
dp1 - m4	3	8.93 ± 0.31 (8.6–9.2)	3.42	20	9.13 ± 0.27 (8.4–9.6)	2.99	–	–	–
dp2 - m3	3	7.47 ± 0.2 (7.24–7.62)	2.7	14	7.49 ± 0.15 (7.16–7.72)	2.02	5	7.14 ± 0.14 (6.93–7.29)	1.92
dp2 - m4	3	8.16 ± 0.04 (8.13–8.2)	0.48	14	8.34 ± 0.32 (7.9–9.32)	3.84	5	7.94 ± 0.16 (7.7–8.15)	2.06
p3 - m3	6	6.79 ± 0.43 (6.32–7.4)	6.37	34	6.86 ± 0.43 (5.54–7.6)	6.23	5	6.22 ± 0.18 (6.07–6.53)	2.89
p3 - m4	6	6.74 ± 0.5 (6–7.24)	7.47*	34	6.69 ± 0.5 (6–7.44)	7.5*	5	7.03 ± 0.13 (6.93–7.24)	1.78
m1 - m3	6	5.63 ± 0.26 (5.36–6.1)	4.56	34	5.43 ± 0.16 (5.1–5.66)	2.99	5	5.34 ± 0.07 (5.26–5.41)	1.23
m1 - m4	6	6.37 ± 0.24 (6.1–6.8)	3.72	34	6.23 ± 0.18 (5.8–6.5)	2.86	5	6.14 ± 0.05 (6.07–6.2)	0.86
Lm1	6	1.97 ± 0.07 (1.88–2.06)	3.42	34	1.87 ± 0.09 (1.7–2.01)	4.82	5	1.82 ± 0.04 (1.78–1.85)	2.12
Wm1	6	0.92 ± 0.02 (0.9–0.94)	2.13	34	0.89 ± 0.07 (0.66–1)	8.18*	5	0.87 ± 0.04 (0.81–0.91)	4.41

**Table 2** External and craniodental measurements of *Rhyncholestes raphanurus* Osgood for pooled samples from Chiloé Island, Chile. Total number of specimens (*n*), mean (*X*), *SD*, minimum and maximum of each variable, and coefficient of variation are presented for each locality. Asterisks indicate Coefficient of Variability (CV) values higher than seven, following Bedeian and Mossholder [34]

Variables	Fundo El Venado			Puerto Carmen – Río Inio		
	<i>n</i>	<i>X</i> ± <i>SD</i> (min - max)	CV	<i>n</i>	<i>X</i> ± <i>SD</i> (min - max)	CV
TTL	9	188.33 ± 19.99 (174–230)	10.62*	3	179.67 ± 8.96 (174–190)	4.99
HBL	9	100.11 ± 12.36 (90–125)	12.35*	3	100.67 ± 8.33 (94–110)	8.27*
TL	9	88.22 ± 9.51 (78–105)	10.78*	3	79 ± 13.53 (65–92)	17.12*
E	9	12.22 ± 0.67 (11–13)	5.45	2	11.5 ± 2.12 (10–13)	18.45*
F	9	21.44 ± 0.73 (20–22)	3.39	3	20.17 ± 0.76 (19.5–21)	3.79
GSL	1	31.1		3	31.7 ± 1.97 (30.35–33.96)	6.2
ZB	1	13.1		3	13.06 ± 1.25 (12.3–14.5)	9.59*
PL	1	18		3	19.02 ± 1.43 (18–20.65)	7.49*
CW	1	2.9		3	3.02 ± 0.22 (2.9–3.28)	7.23*
PWP3	–	–		2	5.56 ± 0.65 (5.11–6.02)	11.62*
PWM1	1	6		3	6.11 ± 0.41 (5.84–6.58)	6.71
PWM3	1	6.4		3	6.52 ± 0.09 (6.43–6.6)	1.34
LINOR	1	6.8		3	6.97 ± 0.1 (6.86–7.06)	1.49
NL	1	15.6		3	16.09 ± 1.28 (15–17.5)	7.96*
BW	1	11.2		3	11.36 ± 0.43 (11–11.84)	3.78
CBL	1	28.2		3	28.79 ± 2.2 (27.36–31.32)	7.62*
BB	1	5.2		3	5.16 ± 0.41 (4.9–5.64)	7.98*
MW	1	1		3	1 ± 0.19 (0.89–1.22)	18.7*
MHp3	–	–		2	2.17 ± 0.45 (1.85–2.49)	20.68*
MHm1	1	2		1	1.8	
MHm3	–	–		2	2.12 ± 0.34 (1.88–2.36)	16.09*
dP1 - M3	1	8.9		3	9.04 ± 0.72 (8.3–9.73)	7.92*
dP1 - M4	1	9.3		3	9.34 ± 0.77 (8.6–10.13)	8.22*
P3 - M3	1	6		3	5.9 ± 0.52 (5.3–6.22)	8.8*
P3 - M4	1	6.4		3	6.24 ± 0.53 (5.65–6.68)	8.53*
M1 - M3	1	4.6		3	4.8 ± 0.19 (4.6–4.98)	3.97
M1 - M4	1	5.1		3	5.21 ± 0.25 (5–5.49)	4.84
LM1	1	1.6		3	1.8 ± 0.12 (1.7–1.93)	6.5
WM1	1	1.4		3	1.38 ± 0.1 (1.3–1.5)	7.52*
LM3	–	–		2	1.46 ± 0.02 (1.45–1.47)	1.23
WM3	–	–		2	1.32 ± 0.04 (1.3–1.35)	2.72
dp1 - m3	1	8.5		1	8.2	
dp1 - m4	1	9.2		1	8.9	
dp2 - m3	–	–		2	7.14 ± 0.18 (7.01–7.26)	2.52
dp2 - m4	–	–		2	7.8 ± 0.28 (7.6–8)	3.64
p3 - m3	1	6.8		3	6.4 ± 0.53 (6.02–7)	8.24*
p3 - m4	1	5.9		3	6.63 ± 0.3 (6.3–6.88)	4.51
m1 - m3	1	5.1		3	5.23 ± 0.11 (5.11–5.3)	2.06
m1 - m4	1	5.8		3	5.94 ± 0.1 (5.82–6)	1.76
Lm1	1	1.8		3	1.81 ± 0.03 (1.78–1.84)	1.74
Wm1	1	0.8		3	0.9 ± 0.09 (0.84–1)	9.66*

**Table 3** Results of a non-parametric Kruskal–Wallis analysis of variance (ANOVA), calculated from Mosimann’s variables, for differences between males and females of *Rhyncholestes raphaunurus* Osgood, for La Picada (Chile), the locality with the largest number of specimens. Total number of specimens ( $n$ ), and specimens by sex (between brackets) are indicated for each measurement. Asterisks mark significant differences (if existent) for sequential Bonferroni-corrected values, following Rice [39]. See text for variable abbreviations

Variable	$n$	H	$P$ -value	Sequential Bonferroni values for $P = 0.05$
TTL	44 (32♂, 12♀)	0.71	0.3987	0.0167
HBL	44 (32♂, 12♀)	0.01	0.9159	0.0500
TL	44 (32♂, 12♀)	4.17	0.0407	0.0100
F	44 (31♂, 12♀)	2.55	0.102	0.0125
E	44 (32♂, 12♀)	0.04	0.8205	0.0250
GSL	30 (20♂, 10♀)	0.56	0.4544	0.0028
ZB	30 (20♂, 10♀)	0.09	0.7579	0.0056
PL	31 (21♂, 10♀)	0.03	0.8657	0.0071
CW	31 (21♂, 10♀)	4.11	0.0395	0.0014
PWP3	12 (7♂, 5♀)	0.01	0.9545	0.0167
PWM1	30 (20♂, 10♀)	0.63	0.4268	0.0025
PWM3	31 (21♂, 10♀)	1.35	0.2405	0.0019
LINOR	32 (22♂, 10♀)	0.03	0.8704	0.0125
NL	31 (21♂, 10♀)	0.55	0.4594	0.0029
BW	31 (21♂, 10♀)	0.1	0.7505	0.0050
CBL	28 (18♂, 10♀)	0.48	0.4867	0.0033
BB	30 (21♂, 9♀)	0	> 0.999	0.0500
MW	32 (22♂, 10♀)	0.57	0.4468	0.0026
MHp3	13 (8♂, 5♀)	2.14	0.1608	0.0016
MHm1	19 (14♂, 5♀)	0.0021	0.9794	0.0250
MHm3	13 (8♂, 5♀)	1.74	0.2028	0.0017
dP1 - M3	32 (22♂, 10♀)	1.49	0.2199	0.0018
dP1 - M4	32 (22♂, 10♀)	1.2	0.2708	0.0020
P3 - M3	32 (22♂, 10♀)	1.69	0.1903	0.0017
P3 - M4	32 (22♂, 10♀)	1.85	0.1716	0.0016
M1 - M3	32 (22♂, 10♀)	0.87	0.3468	0.0023
M1 - M4	32 (22♂, 10♀)	0.26	0.6097	0.0038
LM1	32 (22♂, 10♀)	0.84	0.3559	0.0024
WM1	32 (22♂, 10♀)	3.97	0.0421	0.0014
LM3	13 (8♂, 5♀)	0.09	0.7902	0.0063
WM3	13 (8♂, 5♀)	1.05	0.3349	0.0022
dp1 - m3	19 (14♂, 5♀)	0.48	0.5179	0.0036
dp1 - m4	19 (14♂, 5♀)	0.26	0.6158	0.0042
dp2 - m3	13 (8♂, 5♀)	1.21	0.2968	0.0021
dp2 - m4	13 (8♂, 5♀)	3.35	0.0715	0.0015
p3 - m3	32 (22♂, 10♀)	2.58	0.1076	0.0015
p3 - m4	32 (22♂, 10♀)	0.18	0.6684	0.0045
m1 - m3	32 (22♂, 10♀)	0.03	0.87	0.0100
m1 - m4	32 (22♂, 10♀)	1.35	0.2533	0.0019
Lm1	32 (22♂, 10♀)	0.03	0.8677	0.0083
Wm1	32 (22♂, 10♀)	0.48	0.477	0.0031

**Table 4** Results of a non-parametric Kruskal–Wallis analysis of variance (ANOVA), calculated from Mosimann’s variables for differences between males and females of *Rhyncholestes raphanurus* Osgood, with specimens from all continental localities (i.e., excluding Chiloé Island). The number of analyzed specimens ( $n$ ) and specimens by sex (between brackets) are indicated for each measurement. Asterisks mark significant differences (if existent) for sequential Bonferroni-corrected values, following Rice [39]. See text for variable abbreviations

Variable	$n$	H	$P$ -value	Sequential Bonferroni values for $P = 0.05$
TTL	62 (39♂, 23♀)	0.57	0.4484	0.0125
HBL	62 (39♂, 23♀)	0.06	0.8041	0.0250
TL	62 (39♂, 23♀)	2.96	0.0849	0.0100
F	61 (38♂, 23♀)	0.47	0.486	0.0167
E	62 (39♂, 23♀)	0.03	0.8617	0.0500
GSL	46 (25♂, 21♀)	0.84	0.36	0.0026
ZB	46 (25♂, 21♀)	0.02	0.8947	0.0250
PL	47 (26♂, 21♀)	0.09	0.7644	0.0063
CW	47 (26♂, 21♀)	5.85	0.0148	0.0016
PWM1	23 (9♂, 14♀)	0.18	0.6746	0.0036
PWM3	46 (25♂, 21♀)	0.93	0.3334	0.0025
LINOR	47 (26♂, 21♀)	0.17	0.6771	0.0038
NL	48 (27♂, 21♀)	0.02	0.8767	0.0167
BW	46 (25♂, 21♀)	0.11	0.7398	0.0045
CBL	47 (26♂, 21♀)	0.16	0.6895	0.0042
BB	44 (23♂, 21♀)	0.08	0.7725	0.0071
MW	24 (10♂, 14♀)	1.12	0.2861	0.0023
MHp3	48 (27♂, 21♀)	1.58	0.207	0.0021
MHm1	24 (10♂, 14♀)	0.49	0.4773	0.0029
MHm3	24 (10♂, 14♀)	2.5	0.1117	0.0017
dP1 - M3	46 (25♂, 21♀)	1.8	0.1789	0.0019
dP1 - M4	48 (27♂, 21♀)	1.53	0.2157	0.0022
P3 - M3	48 (27♂, 21♀)	1.94	0.1626	0.0019
P3 - M4	48 (27♂, 21♀)	1.66	0.1967	0.0020
M1 - M3	48 (27♂, 21♀)	0.05	0.8267	0.0100
M1 - M4	48 (27♂, 21♀)	0.03	0.8676	0.0125
LM1	48 (27♂, 21♀)	0.34	0.5581	0.0031
WM1	48 (27♂, 21♀)	9.78	0.0015	0.0014
LM3	48 (27♂, 21♀)	0.93	0.3262	0.0024
WM3	24 (10♂, 14♀)	2.98	0.0739	0.0017
dp1 - m3	24 (17♂, 7♀)	0.1	0.7481	0.0050
dp1 - m4	24 (17♂, 7♀)	0.08	0.7725	0.0083
dp2 - m3	24 (17♂, 7♀)	1.97	0.159	0.0018
dp2 - m4	24 (10♂, 14♀)	7.25	0.007	0.0015
p3 - m3	48 (27♂, 21♀)	7.41	0.0064	0.0015
p3 - m4	48 (27♂, 21♀)	0.34	0.5599	0.0033
m1 - m3	24 (10♂, 14♀)	0.58	0.4471	0.0028
m1 - m4	48 (27♂, 21♀)	3.58	0.0582	0.0016
Lm1	48 (27♂, 21♀)	0.01	0.9332	0.0500
Wm1	48 (27♂, 21♀)	0.1	0.7511	0.0056

**Table 5** Results of a non-parametric Kruskal–Wallis analysis of variance (ANOVA), calculated from Mosimann's variables for differences between continental and Chiloé Island samples of *Rhyncholestes raphaunurus* Osgood. Total number of specimens ( $n$ ), and number of specimens for continental Chile and Chiloé Island are indicated for each measurement. Asterisks mark significant differences (if existent) for sequential Bonferroni-corrected values, following Rice [39]. See text for variable abbreviations

Variable	$n$	$n$ Continental Chile	$n$ Chiloé	H	$P$ -value	Sequential Bonferroni values at $P = 0.05$
TTL	75	62	13	1.27	0.2596	0.0167
HBL	75	62	13	3.44	0.0634	0.0100
TL	75	62	13	1.3	0.2531	0.0125
F	74	61	13	0.44	0.5012	0.0250
E	74	62	12	0.02	0.8782	0.0500
GSL	50	46	4	1.8	0.1799	0.0036
ZB	50	46	4	0.65	0.4208	0.0071
PL	51	47	4	1.64	0.2008	0.0042
CW	51	47	4	1.87	0.169	0.0033
PWP3	25	23	2	1.7	0.1914	0.0038
PWM1	50	46	4	0.12	0.7336	0.0125
PWM3	51	47	4	10.39	0.0012*	0.0014
LINOR	52	48	4	0.18	0.6671	0.0100
NL	8	4	4	3.87	0.0492	0.0021
BW	50	46	4	2.54	0.1105	0.0025
CBL	51	47	4	1.9	0.1674	0.0031
BB	48	44	4	2.1	0.1461	0.0029
MW	26	24	2	2.18	0.1374	0.0028
MHp3	26	24	2	2.30E- 03	0.9615	0.0500
MHm1	26	24	2	1.56	0.203	0.0045
MHm3	26	24	2	0.01	0.923	0.0250
dP1 – M3	50	46	4	4.98	0.0253	0.0019
dP1 – M4	52	48	4	5.78	0.0161	0.0018
P3 – M3	52	48	4	8.72	0.0031	0.0016
P3 – M4	52	48	4	8.62	0.0033	0.0016
M1 – M3	52	48	4	10.2	0.0014*	0.00142
M1 – M4	52	48	4	9.24	0.0023	0.0015
LM1	52	48	4	4.17	0.0399	0.0020
WM1	52	48	4	2.23	0.1306	0.0026
LM3	52	48	4	4.9	0.0249	0.0019
WM3	26	24	2	3.52	0.0538	0.0022
dp1 – m3	26	24	2	0.01	0.9225	0.0167
dp1 – m4	26	24	2	0.19	0.6616	0.0083
dp2 – m3	26	24	2	2.68	0.1013	0.0024
dp2 – m4	26	24	2	3.34	0.0672	0.0023
p3 – m3	52	48	4	1.49	0.2224	0.0050
p3 – m4	52	48	4	1.44	0.2285	0.0056
m1 – m3	52	48	4	6.99	0.0081	0.0017
m1 – m4	52	48	4	8.93	0.0028	0.0015
Lm1	52	48	4	5.94	0.0138	0.0017
Wm1	52	48	4	0.96	0.321	0.0063

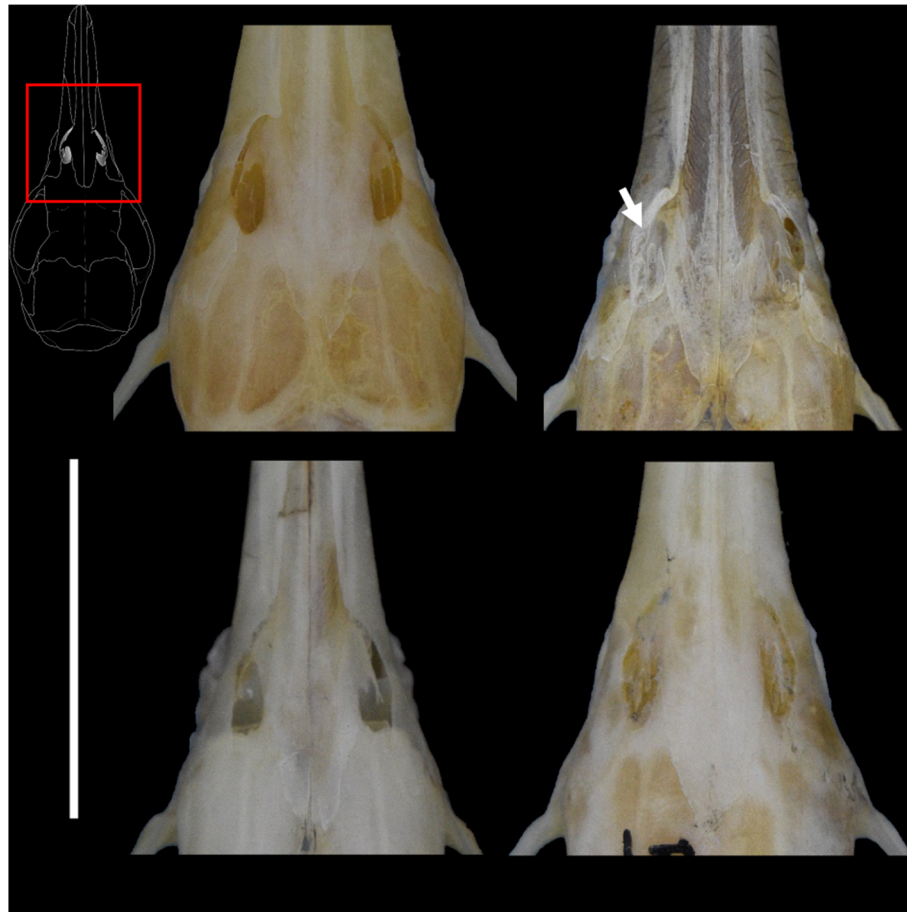


**Fig. 2** Differences in ossification patterns in the anteorbital vacuity in *Rhyncholestes raphanurus* Osgood, from a thin bony cover (top left, FMNH 129823♂), a left closed vacuity in specimen FMNH 127475♂ (top right, white arrow), to partially and fully open in the bottom specimens (FMNH 129834♀, FMNH 129828♀). Scale bar: 1 cm

anteroposterior axis of the crania), frontals show a slight ventrolateral expansion in the orbit, where they contact the alisphenoids. The parietals appear as purely squared, anteriorly delimited by the frontals, ventrolaterally by the alisphenoid, laterally in contact with the squamosal, and posteriorly with the supraoccipital. A well developed and broad nuchal crest was present in adult individuals (e.g., UACH 951♂; UACH 4000♂), less marked in younger individuals with lesser dental wear (e.g., UACH 3999♂, FMNH 129828♀).

In lateral view, nasals extend anteriorly almost to the tip of the premaxillary, forming with the latter the anterior nasal opening. The premaxillary is long and contacts the nasal dorsally until the anteorbital vacuity, and posteriorly with the maxillary. The premaxillary has a thin dorsal spine that extends from a point posterior to dP2 (or to a point between dP2 and P3), contains the four upper incisors, and forms the anterior and half of the lingual wall of the canine alveolus. The maxillary contacts anteriorly with the premaxillary slightly anterior to the anteorbital vacuity,

posterodorsally with the frontal and posteriorly with the lachrymal and yugal bones. A small portion at the ventral part of the orbit region contacts with the orbital process of the palatine bone. It is laterally perforated by the infraorbital foramen, which opens anteriorly above the medial line of M1. The zygomatic arch is weak and curved upwards in its anterior portion. The lateral wall of the yugal has a moderately developed area for the attachment of the *zygomatiscus* muscle sensu [5]. The yugal slightly contacts the lacrimal in the anterior region of the orbit, and with the squamosal half way thru the zygomatic arch; it forms a long spine on the base of the squamosal that extends to the glenoid fossa. The lacrimal is perforated by a single, laterally visible foramen, that opens posterolaterally above the yugal. In the orbital region and as in *Caenolestes* spp., the frontal and alisphenoid are the largest bones at the posterior end (i.e., posterior to the orbital constrictions), while the lacrimal and orbital process of the palatine occupy the anterodorsal and ventral portion of the orbit, respectively. The lacrimal forms the dorsal and upper medial wall for the

orbital canal, the palatine forms the lower medial wall, and the maxillary forms the lateral wall, where this bone develops the zygomatic process. The orbital process of the palatine is wide and goes from anterior to the orbital canal, to posterior of the ethmoidal foramen, but does not contribute to it. Dorsally limited by the frontal and posteriorly by the orbitosphenoid, the parietal has a quadrangular shape and its ventral extension forms part of the floor of the sphenorbital fissure and foramen rotundum. The orbitosphenoid is developed and conspicuous, and is the largest among the extant *Caenolestidae*. It has a semi-quadrangular to circular exposure in the orbital region. The ethmoidal foramen is developed and ventrally orientated, it is formed by the orbitosphenoid ventrally and medially, by the frontal dorsally and laterally, and by the alisphenoid posteriorly. The sphenorbital fissure and foramen rotundum are divided by a bony structure apparently originated at the alisphenoid. The squamosal occupies an important lateral part of the crania, with certain variation in its posterior extension, normally not reaching the nuchal crest and forming the anterior wall of the mastoid foramina (mastoid foramen in Osgood [5]); in some specimens the squamosal reaches the nuchal crest (e.g., UACH 2247♂). As noted by Osgood [5], occipital bones (i.e., supraoccipital, exoccipital, and basioccipital) in adult *Caenolestidae* are seamlessly sutured. However, a very immature specimen of this species (FMNH 129828♀) exhibited the sutures in this complex of bones, which we used to describe this complex of bones not described before for this group (Fig. 3). In occipital

view, the supraoccipital bone is dome-shaped, with its dorsal side limiting with the parietal and sometimes forming a nuchal crest, as described above. This bone forms the dorsal limit of the foramen magnum. The limit between supraoccipital and exoccipital occurs at the level of the mastoid foramen, and runs slightly ventrally towards the foramen magnum, just below its dorsal wall (Fig. 3a). The exoccipitals form the lateral sides of the foramen magnum, and curve ventrally at the base forming the occipital condyles. The limit of the exoccipital bones with the basioccipital runs from posteromedial to anterolateral, contiguous to the most anterior hypoglossal foramen which is completely contained by the exoccipitals (Fig. 3b). The suture between exoccipital and basioccipital runs at the middle of the ventral process of the occipital condyles, from the foramen magnum towards the anterior wall of the jugular foramen. There is no sign of interparietals occurring in this species.

In ventral view, *R. raphanurus* has very large incisive foramina and very large maxillopalatine fenestrae. The palate progressively broadens from dP2 reaching its maximum at M3, and is markedly reduced posteriorly. Incisive foramina generally extend from a point slightly anterior to I3 to an intermediate between dP1 and dP2, or posterior to dP1 (e.g., UACH 2243♂). Maxillopalatine fenestrae extend from a point at half of P3 to a point between M3-M4, or closer to the palatine torus. The separation between maxillopalatine fenestrae is very slender and commonly lost during specimen preparation, which probably led Osgood [9] to describe it as an “open

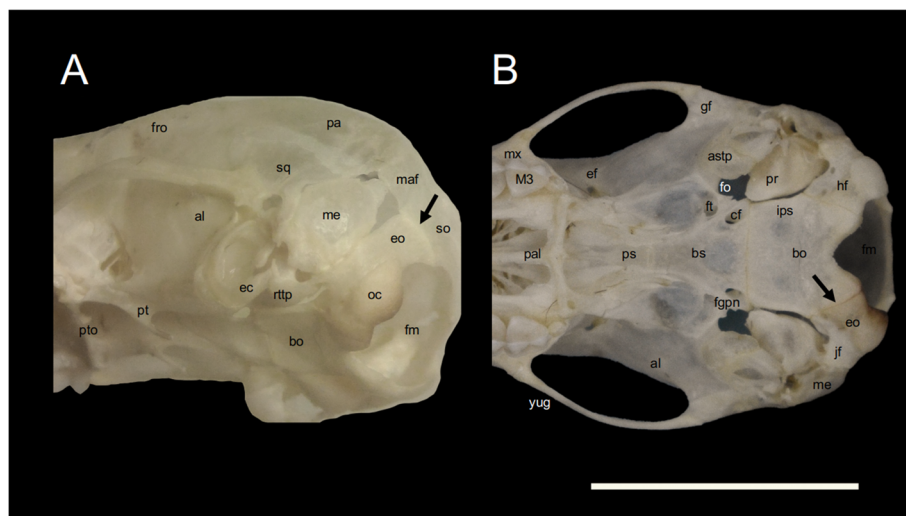


**Fig. 3** Occipital complex and basicranium of *Rhyncholestes raphanurus* Osgood, used to show the sutures between supraoccipital and exoccipital bones (black arrow in A), and exoccipital and basioccipital bones (black arrow in B), based on specimen FMNH 129828♀. Abbreviations: al, alisphenoid; astp, alisphenoid tympanic process; bo, basioccipital; cf., carotid foramen; ec, ectotympanic bone; ef, ethmoidal foramen; eo, exoccipital; fgpn, foramen for the greater petrosal nerve; fm, foramen magnum; fo, foramen ovale; fro, frontal; ft, foramen transversum; gf, glenoid fossa; hf, hypoglossal foramina; ips, inferior petrosal sinus; jf, jugular foramen; M3, third upper molar; maf, mastoid fenestra; me, mastoid exposure of the petrosal bone; mx, maxillary; pa, parietal; pal, palatine; pr, promontorium of the petrosal bone; pt, pterogoid; rtp, rostral tympanic process of the petrosal; so, supraoccipital; sq., squamosal; oc, occipital condyle; pto, palatine torus; yug, yugal. Scale bar: 1 cm

palate". Despite this, several subadult and adult specimens clearly show the bony separation at the middle line (e.g., UACH 2247♂, FMNH 129828♀). They also appear not separated in the drawing made by Patterson y Galardo [6] and their description: "posterior palatal vacuities without median bony partition". Maxillopalatine fenestrae appear commonly separated in other analyzed Caenolestidae as well (see Appendix I). The maxillopalatine fenestrae are mostly limited by the maxillary bones, but by the palatine posteriorly and posterolaterally. The posterior end of the hard palate is formed by the palatine bone, where a well-developed, posteriorly curved palatine torus is formed. The posterior edge of the palate is narrower than the protocones of M3, and the palatine torus is ventrally hypertrophied and is higher at the lateral borders than medially. At the interpalatine suture, the torus has a posteriorly directed pointy process. Two posterolateral palatal foramina are well developed at the most lateral edges of the torus, visible only in oblique ventral views. Medial to these foramina, there are two posterior small foramina, only visible in occipital oblique view, that is the largest among living Caenolestidae and is anterolaterally connected with the posterolateral palatal foramina. The presphenoid is small and located posterior to the choanae opening. This bone is wide at its posterior end but thin and pointy at its anterior end. Anteriorly, it contacts the paired vomer bones, anterolaterally the palatines, laterally the pterygoids, and the basisphenoid posteriorly, in a broad suture. The basisphenoid contacts the basioccipital at the anteriormost point of the promontorium of the petrosal, in a broad mediolaterally directed suture. The tympanic bullae are relatively small, with little vertical (ventral) development of the alisphenoid. At the alisphenoid-petrosal suture, a foramen for the greater petrosal nerve and the foramen ovale are combined in a large foramen (the largest at the posterior region of the cranium), and open widely at the ventral side. The anterior carotid foramen is well developed and opens posteriorly. A well-developed transverse foramen with a bony canal directed laterally, occurs anterior to the carotid foramen at the basisphenoid. At the anterior face of the alisphenoid tympanic process (astp), there is a well-developed canal, with its origin medial to the ventral lux of the foramen ovale, oriented ventrolaterally. In this area, the astp commonly presents a pointy bone process, marking the dorsal-most point of this canal (Fig. 4). This trait is similar to that found in some *Marmosa* spp. [30], page [29], and can be found in old specimens of *Caenolestes* spp. but not in *L. inca*.

#### Mandible

The mandibles are stylized, with a wide (broad) ascending process and a maximum height below m1. The ventral border is straight, not ventrally inflected, and the anterior

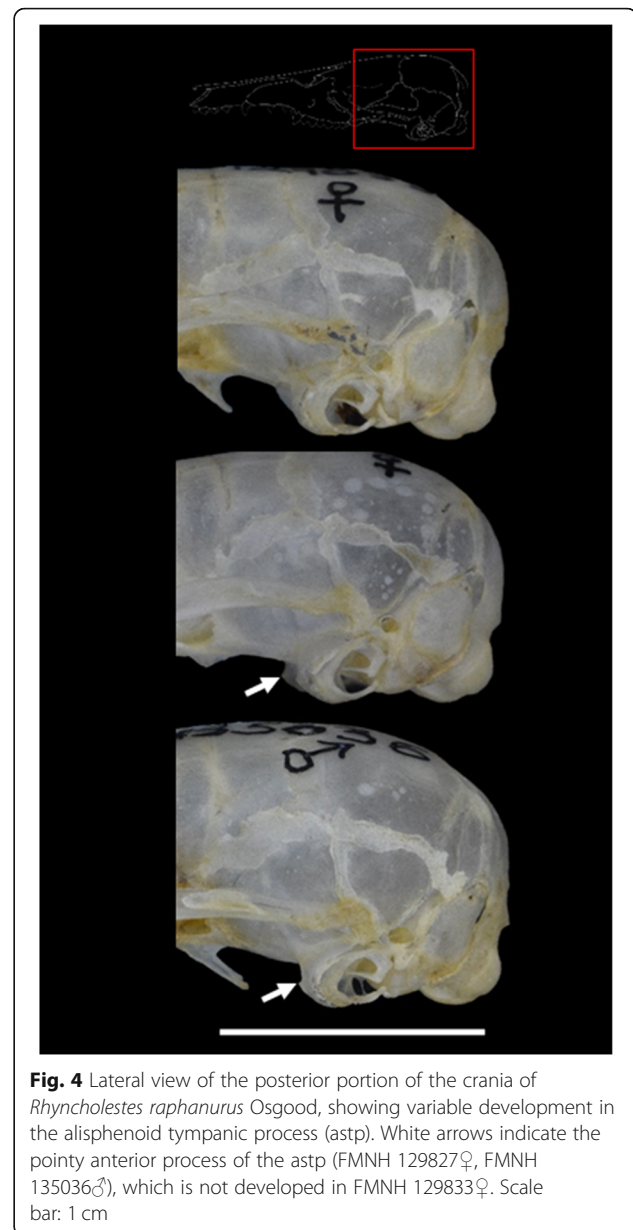


**Fig. 4** Lateral view of the posterior portion of the crania of *Rhyncholestes raphanurus* Osgood, showing variable development in the alisphenoid tympanic process (astp). White arrows indicate the pointy anterior process of the astp (FMNH 129827♀, FMNH 135036♂), which is not developed in FMNH 129833♀. Scale bar: 1 cm

region becomes dorsoventrally narrow anterior to p3, reaching its minimum in the opening of the alveolus for the procumbent incisor. The mandible has two or three mental foramina, the first one under p3 and the other/s between m1–2 (e.g., two foramina in UACH 4000♂; three in the left side of UACH 948♂). The coronoid process and the mandibular body (i.e., the portion that contains the teeth) form an almost 90° angle. The coronoid crest is well-developed at the anteroventral portion, gradually fading towards its dorsal edge. Some specimens present a totally faded coronoid crest at approximately the middle height of the coronoid process (e.g., FMNH 127467♂), whereas others present a continuously conspicuous crest until the apex of the coronoid

process (e.g., FMNH 127471♀). The ventral crest of the masseteric fossa is evenly developed throughout its length.

### Dentition

Several dental traits are unique to *R. raphanurus*: 1) the bilobed upper incisors (I2–4), with a large notch separating the anterior blade-like from the posterior peg-like cusps; 2) the broad diastemas between I4–C1, C1–dP1, dP1–dP2, and dP2–P3–M4; 3) the well-marked reduction of M4 (compared to *Caenolestes* and *Lestoros*); 4) the greater size of the procumbent first lower incisors, relative to the other teeth; and 5) the greater reduction of the four lower incisor-like teeth after the procumbent lower incisor. Also, the spatial arrangement of the upper teeth of *R. raphanurus* and its diastemas are unique, with upper incisors from I1 to I3 in contact, I3 separated from I4 by a diastema half the length of I4 (approximately), I4 separated from C1 by a large diastema, which is slightly shorter than the one separating C1 from dP1 (the largest diastema); dP1 and dP2 are separated by a diastema similar in size to that separating I4 from C1, dP2 is either very close or in contact with P3, and there is no other diastema in the upper tooth-row.

**Incisors.** All three first upper incisors have a wide crown and are in contact with the preceding and posterior tooth. As with the rest of other living caenolestids, the first two incisors are not separated from the posterior ones by a diastema, as it occurs in all? living didelphids. The first upper incisors are lingually concave, somewhat “closing” the buccal cavity with the inferior procumbent incisors. The following incisors (I2–4) are large, bucco-lingually flattened and oriented in a mesiodistal axis. These teeth in *R. raphanurus* have a unique shape: “...upper incisors with a broad anterior blade and a blunt, slightly curved, posterior cusp, the two parts separated by a deep cleft...” Osgood [9] p. [169]. The third and fourth incisors are separated by a diastema, which is also present in *L. inca*, but in *R. raphanurus* the distance between I3–4 is shorter than that between I4–C1.

First lower incisors share the same pseudodiprotodont pattern characteristic of Paucituberculata, with the two hypertrophied and strongly procumbent. Each procumbent incisor is followed in each mandible by 3 small peg-like teeth which are undistinguishable between themselves, and are supposed to represent i2–3 and c1. Additionally, the hypertrophied procumbent incisors show a clear pattern of wear related to the specimen size and, allegedly, age; small individuals with little tooth wear have a dorsal cutting edge that goes from base to the tip of the tooth. Contrary to this, large individuals with highly worn teeth show this same cutting edge restricted to the last quarter of the procumbent tooth, while the base is cylindrical in transverse section. The two latter cases are the extreme points of a continuum, related to the apparent continuous growth of these teeth.

**Canines.** The upper canine in *R. raphanurus* has been described as sexually dimorphic, “premolariform” in females and “caniniform” in males [9], somewhat implying single rooted canines in males, and double rooted in females. Although consistent in the majority of the specimens analyzed for this character (i.e., 23♀ and 30♂), we observed variation in the upper canine shape: seven males (23%) presented a premolar-like shape, while some females (17%) presented the typical, male-like canine shape (Fig. 5).

Lower canines (if present) are small and incisor-like and without marked cingula, in specimen IEEUACH 3578♂ appears to be double-rooted.

**Premolars.** Upper premolars increase in size from dP1 to P3, with a diastema between C1–dP1, dP1–dP2, and dP2–dP3; dP3 forms a continuum with M1–4. In occlusal view, the highest cusp in each premolar is shifted/moved posteriorly: in dP1, the major cusp is anteriorly located; in dP2 it is medially located; and in P3 the major cusp is displaced posteriorly. This “progression” is not as marked as in other living caenolestids (e.g., *Lestoros inca* AMNH 42685♀; *Caenolestes fuliginosus* MACN 31.143♀, MACN 31.144♂), where the first two premolars have the central cusp in the anterior or medial region of the tooth. A similar pattern to the one present in *R. raphanurus* (but not as well marked) was observed in *C. caniventer* (e.g., AMNH 47175♂). *Rhyncholestes raphanurus* shows a unique pattern of occlusal shape in upper premolars, with a well-marked talon in dP1 and a posterior cusp; an even occlusal surface in dP2 with an anterior and posterior cingula and talon, respectively; and a well-marked cingulum in P3 with a large anterior cusp and a very large posterior cusp. The largest cusp in P3 has a well-developed posterior cutting blade, which forms a continuous cutting blade with the highly developed StB of M1. In lateral view, dP1 is as tall as I4 and with a similar shape but a sharper central cusp. The next upper premolar (dP2) is larger than dP1 and has a symmetric shape, both in occlusal and lateral views (i.e., the main cusp is roughly located at half the tooth). Finally, P3 is the tallest tooth in the upper tooth-row, with a robust anterior cingula and no talon, the posterior crest is in direct contact with M1’s parastylar corner. Also, P3 is obliquely implanted with respect to the antero-posterior axis of the crania, which coincides with the point where the palate broadens.

Lower premolars greatly increase in size from dp2 to p3, they are similar in general shape but p3 is twice the size of dp2 and has a well-developed, wider talon than in dp2.

**Molars.** The general shape of upper molars in *R. raphanurus* is quadrangular, with a progressive (from M1 to M3) narrowing of the posterior area of each tooth. Molars have a quadrangular general shape, with a progressive narrowing (from M1 to M3) of the posterior portion of each molar in which StD + metacone become closer to the



**Fig. 5** Canine type variation in specimens of *Rhyncholestes raphanurus* Osgood showing the typical male-like canine (FMNH 50071♂, top left; FMNH 124003♀, top right), an intermediate, almost premolariform canine (FMNH 129831♀, bottom left), and a typical female-like, premolariform canine (FMNH 129834♀, bottom right). Scale bar: 1 cm

metaconule, and a reduced basin of the area between metaconule and metacone. The first two upper molars are subequal in size, rectangular in occlusal shape, while M3 is reduced and M4 is a very small single-rooted tooth, smaller than any other tooth including the incisors and circular in occlusal view. The first two upper molars have a well-marked metaconule, which is reduced in M3. In the first two upper molars StD is the highest cusp, almost as tall as the main cusp of P3. The first upper molars have a well-marked labial cingulum, M1–2 have a lingual cingulum between protocone and metaconule, reduced or absent in M3. In general, the last upper molar has two poorly developed cusps, but sometimes this tooth can have a single, central cusp.

Lower molars are subequal in size from m1 to m3, m4 being notoriously reduced in both occlusal and lateral views. The trigonid is short (i.e., mesiodistally compressed) in the first three molars, with a well-marked anterior cingulum that is narrower in m1, wider in m2 and slightly narrow in m3. The talonid is wider than the trigonid in m1–2, equally wide in m3. The trigonid is open in its lingual side in the first three molars, with a lingual cingulum that reaches the base of the metaconid in m2–3 but is continuous and joins the lingual crest running mesially from the metaconid in m1. In occlusal view, the metaconid becomes progressively closer to the paraconid from m1 to m3 reducing the trigonid area, with a change

in the orientation of the postprotocristid from oblique to mostly transversal in relation to the tooth row. This pattern is less marked than in *C. fuliginosus* (e.g., MACN 31.143♀, MACN 31.144♂). The cristida obliqua is well developed and reaches the protoconid, closing the talonid in its labial side. The lingual side of the molars in the talonid are open, just like in the trigonid. The entoconid is slightly projected lingually, especially in m2–3. Two crests form a well-developed basin between entoconid and metaconid, labially limited by a crest that originates in the entoconid and reaches the posterior wall of the trigonid. This basin reduces its size from m1 to m3, along with the mesiodistal reduction in molar size. The posterior “wall” of m1–m3 is closed by the post-hypoconid crest, that is well marked in m1 and less so in m3. A clearly developed hypoconulid is present in m3 but not so in m1–2, in a progression from poorly developed to well-developed hypoconulid (e.g., FMNH129828♀). The last molar is a very small tooth with well-marked trigonid and talonid, separated by a well-developed metaconid, the only cusp that can be clearly identified in this molar. Although m4 can have the appearance of being single rooted in some specimens (e.g., IEEUACH 4522♀; IEEUACH 2250♀) or double rooted in others (e.g., IEEUACH 2244♂; IEEUACH 2247♂; MACN 20625♂), all the toothless specimens we observed showed two alveoli.

## Discussion

In this work, we presented an extensive revision of the morphologic and morphometric variability and variation of the great majority of *R. raphanurus* specimens deposited in mammal collections. Our sample comes from a few scattered localities throughout what has been inferred to be the species range [3], showcasing how poorly represented this marsupial is in mammal collections throughout the world, and how little we know even after almost 100 years of its original description.

Despite some limited samples, most external measurements presented the highest variability within sampled localities (Tables 1 and 2), a similar trend to what was described for *Lestoros inca* and other New World marsupials [7, 11, 24]. On the other hand, craniodental measurements showed the lowest within-locality variability, especially in samples with  $n > 5$ , with the exception of mandibular width and height (Tables 1 and 2), which are variables directly related to individual growth and, for the latter, a positive allometric change was described [4, 22]. Our data shows that a small number of individuals in this species, depending on the trait, might not be enough to “capture” the local or regional variability (e.g., dP1-M3, dP1-M4, in the samples from Río Inio, Chiloé). Others show an intraspecific variability related to sexual dimorphism (e.g., M1 in continental samples; Table 4), or a small sample that was constrained towards an extreme within the variability (e.g., M1–3 and width of M3 in the sample from Chiloé; Table 5, and Additional file 1). As discussed in Martin [24] for *D. gliroides*, a marsupial living in a very similar area (albeit more extended in its distribution) than *R. raphanurus*, variability can be underrated when small samples of specimens are analyzed, not showing the amount of change within a population, see also [4, 42, 43].

Despite the significant differences found in the ANOVA between continental and insular specimens (Table 5), all measurements fall well within the range of continental samples (Tables 1 and 2). The smaller average sizes of some dental measurements compared in the ANOVAs might be an artifact of the small sample size, which is also shown in the very large CV values (usually, CV values for dental measurements in marsupials are  $< 4$ , showing little variation/dispersion [7, 11, 44]);). Similar results, in which no difference was found between Island and continental populations, were described for another marsupial (*Dromiciops gliroides* [7, 21];), sigmodontine rodents (e.g., *Geoxus* spp., [45]; *Abrothrix manni* [46]), and a carnivore (*Lycalopex fulvipes*, [47]). Despite differences in the biogeographic history of the taxa mentioned above, these results appear to be a consequence of the geological history of the area, where the northwestern portion of Chiloé Island remained in contact with the rest of the continent until recent times (while the rest of the Island was covered by glacial ice) [48, 49], which does not appear to be enough time to have produced isolation in these species.

Our data shows that sexual dimorphism in this species is only restricted to canine form, and not to size or shape (externally and craniodentally, see also Additional file 1), with similar results described by Martin [11] for a linear morphometric analysis, and by Astúa [23] for sexual size and sexual shape dimorphism analyses. Oddly, Osgood [9] described the shape difference between male and female canines, but our examination of the type specimen (a female) showed a premolariform canine in the left side [9: p. 173; PL XXIII], but a male-like canine on the right side. We found the premolariform condition in females and typical canine form in males is present in 80% of the samples with no relation to locality, offering evidence that canine sexual dimorphism is a distinctive character of *R. raphanurus*, and that this variation is not related to differences between mainland and insular forms. Canine sexual dimorphism was also described for *C. fuliginosus* [8, 50], but differences in crown shape, and especially accessory cusps were less developed than in *R. raphanurus*.

We herein described (for the first time to our knowledge) some morphologic characters including the occipital complex (Fig. 3; previously considered as fused bones [5, 9]) or the presence/absence of interparietal bones see [51]. The absence of an interparietal bone can be considered an autapomorphic characteristic of Caenolestidea, as it appears to be absent only in this group of marsupials. Similarly, other characters previously studied as the form of the subsquamosal foramen or the position of sphenorbital foramen relative to the palatine fenestra, see [17], were found to be polymorphic in this species, and should be treated with caution when studying small samples, which might not reflect the full extent of the species variability and variation. Finally, as noted before by Martin [7], there is a marked variation in some traits in the species of Caenolestidae which can be used as a framework when studying and describing fossils forms of this group. Achieving clarity in the way these traits vary is desirable when creating robust morphological matrices for phylogenetic hypothesis, and comparisons between groups. In this sense, studies that use large series of specimens and detailed descriptions of morphology, e.g., [7, 24, 29, 32, 44], this work are important in comparative morphology and hypothesis-driven studies on the evolution of New World marsupials.

We found a series of cranial traits unique to *R. raphanurus* not present in extant Caenolestidae: 1) the maxillary process of the incisive fenestra ridge is wide anteriorly and narrows posteriorly; 2) the post torus palatal foramen is large and laterally connected with the minor palatine foramen; 3) the orbitosphenoid exposure is wide and occupies a big part of the orbital region; 4) the premaxillary is twice wider than tall; 5) a broad anterior interorbital region, that is as broad as the interlacrimal region; and 6) a straight lateral aspect of the premaxillary at the anterior nasal aperture. These characters might be an indication of a unique,

separate evolutionary path taken by *R. raphanurus* when compared to the other two living genera (*Caenolestes* and *Lestoros*) which, despite being clearly different [7], appear closer morphologically. Unfortunately, we are unable to compare most of our cranial descriptions with fossil Caenolestidae, since most specimens are commonly represented by tooth remains (some with partial mandibles).

A recent review of Paucituberculata done by Abello [31] considered the antemolar formula of caenolestids to have eight teeth, assigned to four incisors, a canine and three premolars, a number that is not supported by this study and those of Martin [7, 52]. Despite some anomalies described in Martin [7, 52], most of the specimens we studied show seven antemolar teeth, with the presence of three incisors (including the procumbent one), a canine and three premolars. Even when homologies of the anterior, incisor-like teeth cannot be confirmed, the most common number is seven, with six and eight antemolar teeth registered in some anomalous specimens. Assuming a common pattern of eight antemolar teeth implies the loss of two dental units in specimens with six teeth. The easiest and most parsimonious “solution” would be to have seven teeth and lose or gain one unit in specimens with six or eight antemolar teeth, respectively. This process has no implications on the supposed ancestral dental formula in caenolestids since a reversion to eight molars from the common formula of seven (as in some specimens), could be referred to as an atavism [52]. In sum, we here propose that the dental formula for living and extinct caenolestids (i.e., family Caenolestidae) would be I4/i3 C1/c1 dP1–2/dp1–2 P3/p3 M4/m4.

Future studies of *R. raphanurus* using different methods as geometric morphometrics or micro computed tomography could add new information on the variability and variation of the species. We also expect new specimens from other localities, especially from Argentina and Chiloé Island, could provide an opportunity to complement and/or test our results, adding information on several aspects of the species morphology and ecology.

## Conclusions

Comparative studies of continental and Chiloé Island specimens support the treatment of *R. raphanurus* as a single valid species. Morphometric differences found between Chiloé and continental forms differ mostly in a similar degree/or within the extremes of different continental populations (Tables 1 and 2, and Additional file 1). Altogether, the morphology of *R. raphanurus* diverges from other extant Caenolestidae in a greater degree than *Lestoros* and *Caenolestes* differ. For example, the elongated premaxillary, the deeply bilobed incisors, the reduced M4 and other traits, are discrete differences of this genus. Nevertheless, the convergence of some characters with the genus *Caenolestes* might reflect similar feeding constraints, and are not in agreement with some phylogenetic hypothesis proposed before [17, 31,

32], where *Lestoros* and *Rhyncholestes* appear as sister taxa. For example, the bilobed incisors are found also in *C. caniventer*, although to a lesser degree, and the pointy process at the anterior face of the astp is only found in *Caenolestes* spp., while it is absent in *Lestoros*. A wider comparison (between genera and species), and new genetic data or new methods (e.g., geometric morphometrics) could provide new insights into these phylogenetic questions.

The information presented herein can be used in anatomical and paleontological studies dealing with caenolestids in particular and marsupials in general, also providing a sound basis for anatomical inferences made from fossils. Further studies contributing with more information from morphological traits (e.g., number of teats, postcranium, embryos) could shed some light on the relationships of these unique and understudied taxa.

## Appendix

### Appendix I. List of analyzed specimens.

*Rhyncholestes raphanurus*. Argentina. Río Negro Province; Parque Nacional Nahuel Huapi, Puerto Blest (MACN 20625, MMP 4055). Chile. Osorno Province; Maicolpué, 65 km W Osorno and 2 Km S Bahía Mansa (FMNH 129828); 32 Km SSE Osorno, 15 Km NNW Pto Octay (FMNH 129833); Comuna Entre Lagos, Puyehue (IEEUACH 3998-IEEUACH 4000); Puyehue National Park, 9.4 Km NW Antillanca and 7.4 km SE Aguas Calientes (FMNH 124002-FMNH 124003); Los Mallines, 9.4 Km W of ski center at Antillanca (FMNH 129827); Llanquihue Province; Comuna Puerto Octay, La Picada (BMNH 75.1723 [4 Km E], IEEUACH 947-IEEUACH 952, IEEUACH 2241-IEEUACH 2247, IEEUACH 2249-IEEUACH 2250, IEEUACH 2252, IEEUACH 3576, IEEUACH 3578, FMNH 124004, FMNH 127467-FMNH 127475, FMNH 129823-FMNH 129824, FMNH 129830); Refugio Volcán Osorno, La Picada (FMNH 50071); Parque Nacional Vicente Perez Rosales, (IEEUACH 4522); Palena Province; 19.7 km N Río Negro and 26.7 km S Contao (FMNH 129831); 11.1 Km WNW Río Negro and 35.3 Km SSW Contao (FMNH 129834, FMNH 129836); 12.4 km WNW Río Negro and 34 km S Contao, Carretera Austral, (FMNH 135035, FMNH 135036); Chiloé Province; Palomar, Fundo El Venado (IEEUACH 1831, IEEUACH 1835); Puerto Carmen (IEEUACH 1840); Río Inio (FMNH 22422, FMNH 22423). For a list of *Caenolestes* spp. and *Lestoros inca* studied specimens see González Chávez et al. [8], and Martin [7], respectively.

## Supplementary information

Supplementary information accompanies this paper at <https://doi.org/10.1186/s40693-020-00089-6>.

**Additional file 1.** Results of the full model Principal Component Analysis, and the Principal Component Analyses generated with Mossimann variables for external, selected cranial and dental measurements.

**Acknowledgments**

Curators Robert Voss (AMNH), Paula Jenkins (BMNH), Bruce Patterson (FMNH), Milton Gallardo/Guillermo D'Elia (UACH), David Flores/Pablo Teta (MACN) and Alfred Gardner (USNM) allowed access to specimens under their care. Linda Gordon (USNM) and John Phelps (FMNH) went beyond their normal duties to assist GMM during his visits to the institutions in which they work at. GMM's visit to the AMNH was funded by a Collection Study Grant, BGC's visits to FMNH and NMNH were funded by grants given by each institution. Eugene Watkins and Michael Simeon provided economic support during parts of this study. Cecilia Brand provided insightful comments on statistical tests and analyses. Part of this work was done during the doctoral thesis of GMM, and benefited from comments by Francisco Goin, David Flores, Analía Forasiepi and Adriana Candela (the last three acted as referees) We thank Prof. Eduardo Palma for inviting us to participate in this special number on the Ecology and Evolution of South American marsupials.

**Authors' contributions**

GMM designed the study. BG and GMM collected the data. GMM, BG and FB analyzed the data and wrote the manuscript. The author(s) read and approved the final manuscript.

**Funding**

Not applicable

**Availability of data and materials**

All data generated or analyzed during this study are included in this published article [and its supplementary information files].

**Ethics approval and consent to participate**

Not applicable.

**Consent for publication**

Not applicable.

**Competing interests**

The authors declare that they have no competing interests.

Received: 28 October 2019 Accepted: 23 March 2020

Published online: 07 April 2020

**References**

- Tyndale-Biscoe CH. Life of marsupials. 1st ed. Collingwood: CSIRO Publishing; 2005.
- Patterson BD. Order Paucituberculata. In: Wilson DE, Mittermeier RA, editors. Handbook of the mammals of the world volume 5 Monotremes and marsupials. Barcelona: Lynx Edicions; 2015. p. 188–97.
- Martin GM. Geographic distribution of *Rhyncholestes raphanurus* Osgood, 1924 (Paucituberculata: Caenolestidae), an endemic marsupial of the Valdivian temperate rainforest. *Aust J Zool.* 2011;59:118–26.
- Yablokov AV. Variability of mammals. 1st ed. New Delhi: Amerind Publishing; 1974.
- Osgood WH. A monographic study of the American marsupial *Caenolestes*. *Fieldiana Zool.* 1921;16:1–162.
- Patterson BD, Gallardo MH. *Rhyncholestes raphanurus*. *Mamm Species.* 1987;286:1–5.
- Martin GM. Intraspecific variability in *Lestoros inca* (Paucituberculata, Caenolestidae), with reports on dental anomalies and eruption pattern. *J Mammal.* 2013;94:601–17.
- González Chávez B, Rojas-Díaz V, Cruz-Bernate L. Demographic parameters of the silky shrew-opossum *Caenolestes fuliginosus* (Paucituberculata, Caenolestidae) along an altitudinal gradient in the cordillera central of the Colombian Andes. *J Mamm Evol.* 2019;26:39–50.
- Osgood WH. Review of living caenolestids with description of a new genus from Chile. *Fieldiana Zool.* 1924;14:165–73.
- Gallardo MH. Hallazgo de *Rhyncholestes raphanurus* (Marsupialia, Caenolestidae) en el sur de Chile. *Arch Biol Med Exp. (Santiago).* 1978;2:181.
- Martin G. M. Sistemática, distribución y adaptaciones de los marsupiales Patagónicos. Ph.D. dissertation, Universidad Nacional de La Plata, La Plata, Argentina. 2008.
- Meserve PL, Murúa R, Lopetegui NO, Rau JR. Observations on the small mammal fauna of a primary temperate rain forest in southern Chile. *J Mammal.* 1982;63:315–7.
- Patterson BD, Meserve PL, Lang BK. Distribution and abundance of small mammals along an elevational transect in temperate rain forests of Chile. *J Mammal.* 1989;70:67–78.
- Morton SR. Ecological correlates of caudal fat storage in small mammals. *Australian Mamm.* 1980;3:81–6.
- Kelt DA, Martínez DR. Notes on the distribution and ecology of two marsupials endemic to the Valdivian forests of southern South America. *J Mammal.* 1989;70:220–4.
- Nilsson MA, Churakov G, Sommer M, Van Tran N, Zemann A, Brosius J, Schmitz J. Tracing marsupial evolution using archaic genomic retroposon insertions. *PLoS Biol.* 2010;8(7):e1000436. <https://doi.org/10.1371/journal.pbio.1000436>.
- Ojala-Barbour R, Pinto CM, Brito JM, Albuja LV, Lee JRTE, Patterson BD. A new species of shrew-opossum (Paucituberculata: Caenolestidae) with a phylogeny of extant caenolestids. *J Mammal.* 2013;94:967–82.
- Bublitz J. Untersuchungen zur Systematik der rezenten Caenolestidae Trouessart, 1898: unter Verwendung craniometrischer Methoden. *Bonn Zool Monogr.* 1987;23:1–96.
- Patterson BD. Genus *Rhyncholestes* Osgood, 1924. In: Gardner AL, editor. Mammals of South America, volume 1: marsupials, xenarthrans, shrews, and bats. Chicago: University of Chicago Press; 2007–2008. p. 126–7.
- Wilson DE, Reeder DAM. Editors. Mammal Species of the World. A Taxonomic and Geographic Reference (3rd ed.), Johns Hopkins University Press. 2005: 2,142 pp.
- Suarez-Villota E, Quercia CA, Nuñez JJ, Gallardo MH, Himes CM, Kenagy GJ. Monotypic status of the south American relictual marsupial *Dromiciops gliroides* (Microbiotheria). *J Mammal.* 2018;99:803–12.
- Flores DA, Abdala F, Martin GM, Giannini NP, Martínez JM. Post-weaning cranial growth in shrew opossums (Caenolestidae): a comparison with bandicoots (Peramelidae) and carnivorous marsupials. *J Mamm Evol.* 2014;22:1–19.
- Astúa D. Cranial sexual dimorphism in New World marsupials and a test of Rensch's rule in Didelphidae. *J Mammal.* 2010;91:1011–24.
- Martin GM. Intraspecific variability and variation in *Dromiciops* Thomas 1894 (Marsupialia, Microbiotheria, Microbiotheriidae). *J Mammal.* 2018;99:159–73.
- Bateson W. Materials for the study of variation. 1st ed. Baltimore: Johns Hopkins University Press; 1939.
- Simpson GG. Tempo and mode in evolution. 1st ed. New York: Columbia University Press; 1994.
- Wagner GP, Altenberg L. Perspective: complex adaptations and the evolution of evolvability. *Evolution.* 1996;50:967–76.
- Wagner GP, Booth G, Bagheri-Chaichian H. A population genetic theory of canalization. *Evolution.* 1997;51:329–47.
- Wible JR. On the cranial osteology of the short-tailed opossum *Monodelphis brevicaudata* (Didelphidae, Marsupialia). *Ann Carnegie Mus.* 2003;72:137–202.
- Voss RS, Jansa SA. Phylogenetic studies on didelphid marsupials II. Nonmolecular data and new IRBP sequences: separate and combined analyses of didelphine relationships with denser taxon sampling. *Bull Am Mus Nat Hist.* 2003;276:1–82.
- Abello MA. Sistemática y bioestratigrafía de los Paucituberculata (Mammalia: Marsupialia) del Cenozoico de América del Sur. Ph.D. dissertation, Universidad Nacional de La Plata, La Plata, Argentina. 2007.
- Abello MA. Analysis of dental homologies and phylogeny of Paucituberculata (Mammalia: Marsupialia). *Bio J Linn Soc Lond.* 2013;109:441–65.
- Lockett PW, Hong N. Ontogenetic evidence for dental homologies and premolar replacement in fossil and extant caenolestids (Marsupialia). *J Mamm Evol.* 2000;7:109–27.
- Bedeian AG, Mossholder KW. On the use of the coefficient of variation as a measure of diversity. *Organ Res Methods.* 2000;3:285–97.
- Mossimann JE. Size allometry: size and shape variables with characterizations of the lognormal and generalized gamma distributions. *J Am Stat Assoc.* 1970;65:930–45.
- Maechen-Samuels J, Van Valkenburgh B. Forelimb indicators of prey-size preference in the Felidae. *J Morphol.* 2009;270:729–44.
- Morales MM, Giannini NP. Morphofunctional patterns in Neotropical felids: species co-existence and historical assembly. *Bio J Linn Soc Lond.* 2010;100: 711–24.
- Schiaffini MI, Prevosti FJ, Ferrero BS, Noriega JI. A Late Pleistocene Guloninae (Carnivora, Mustelidae) from South America (Argentina, Entre Ríos province), biogeographic implications. *J S Am Earth Sci.* 2017;78:141–9.

39. Rice WR. Analyzing tables of statistical tests. *Evolution*. 1989;43:223–5.
40. Di Rienzo JA, Casanoves F, Balzarini MG, González L, Tablada M, Robledo CW. InfoStat versión 2010. Grupo InfoStat, FCA, Universidad Nacional de Córdoba, Córdoba, Argentina. 2010.
41. Cattell RB. The scree test for the number of factors. *Multivariate Behav Res*. 1966;1:245–76.
42. Simpson GG, Roe A, Lewontin RC. *Quantitative zoology*. Revised ed. New York: Dover Publications; 2003.
43. Zachos FE, Apollonio M, Bärmann EV, Festa-Bianchet M, Göhlich U, Habel JC, Haring E, Kruckenhauser L, Lovari S, McDevitt AD, Pertoldi C, Rössner GE, Sánchez-Villagra MR, Scandura M, Suchentrunk F. Species inflation and taxonomic artefacts-acritical comment on recent trends in mammalian classification. *Mamm Biol*. 2013;78:1–6.
44. Martin GM. Intraspecific variation in *Lestodelphys halli* (Marsupialia: Didelphimorphia). *J Mammal*. 2005;86:793–802.
45. Teta P, D'Elía G. Taxonomical notes on the long-clawed mole mice of the genus *Geoxus* (Cricetidae), with the description of a new species from an oceanic Island of southern Chile. *Hystrix*. 2016; <http://www.italian-journal-of-mammalogy.it/article/view/11996/pdf>.
46. D'Elía G, Teta P, Upham NS, Pardiñas UFJ, Patterson BD. Description of a new soft-haired mouse, genus *Abrothrix* (Sigmodontinae), from the temperate Valdivian rainforest. *J Mammal*. 2015;96:839–53.
47. Jiménez JE. Ecology of a coastal population of the critically endangered Darwin's fox (*Pseudalopex fulvipes*) on Chiloé Island, southern Chile. *J Zool*. 2007;271:63–77.
48. Villagrán C, Moreno P, Villa R. Antecedentes palinológicos acerca de la historia cuaternaria de los bosques chilenos. In: Armesto JJ, Villagrán C, Arroyo MK, editors. *Ecología de los bosques nativos de Chile*. Santiago de Chile: Editorial Universitaria; 1997. p. 51–69.
49. Villagrán C, Hinojosa LF. Esquema biogeográfico de Chile. In: Llorente Bousquets J, Morrone JJ, Editors. *Regionalización Biogeográfica en Iberoamérica y tópicos afines México*: Jiménez Editores; 2005. p.551–577.
50. Albuja VL, Patterson BD. A new species of northern shrew-opossum (Paucituberculata: Caenolestidae) from the cordillera del Cóndor, Ecuador. *J Mammal*. 1996;77:41–53.
51. Beck RMD, Taglioretti ML. A nearly complete juvenile skull of the marsupial *Sparassocynus derivatus* from the Pliocene of Argentina, the affinities of "Sparassocynids", and the diversification of opossums (Marsupialia; Didelphimorphia; Didelphidae). *J Mamm Evol* 2019; <https://doi.org/https://doi.org/10.1007/s10914-019-09471-y>.
52. Martin GM. Dental anomalies in *Dromiciops gliroides* (Microbiotheria, Microbiotheriidae), *Caenolestes fuliginosus* and *Rhyncholestes raphanurus* (Paucituberculata, Caenolestidae). *Rev Chil Hist Nat*. 2007;80:393–406.

## Publisher's Note

Springer Nature remains neutral with regard to jurisdictional claims in published maps and institutional affiliations.

**Ready to submit your research? Choose BMC and benefit from:**

- fast, convenient online submission
- thorough peer review by experienced researchers in your field
- rapid publication on acceptance
- support for research data, including large and complex data types
- gold Open Access which fosters wider collaboration and increased citations
- maximum visibility for your research: over 100M website views per year

**At BMC, research is always in progress.**

Learn more [biomedcentral.com/submissions](https://biomedcentral.com/submissions)

